PRINTED IMAGE WATERMARKING USING DIRECT BINARY SEARCH HALFTONING

Fuping Wang[1], and Jan P. Allebach[2]

[1]State Key Laboratory of Power System and Generation Equipment, Tsinghua University, Beijing 100084, China (wangfuping97@mails.tsinghua.edu.cn)
[2]School of Electrical and Computer Engineering, Purdue University, West Lafayette, IN 47907 USA (allebach@purdue.edu)

ABSTRACT

A novel framework using direct binary search (DBS) is proposed for printed image watermarking. Watermarks are embedded in the halftone by forcing pairs of pixels to be positively or negatively correlated, halftone image quality and watermark detection are two goals to be jointly maximized, and a modified toggle and swap strategy of DBS is employed to find the optimal halftone. Experiment results are presented for watermark rate (WMR) equal to 4.62%, 9.77%, 27.81%, and 46.73%. Excellent performance is demonstrated, e.g. when the WMR is below 10%, the image quality degradation is negligible, and the error rate (BER) is about 1%.

Index Terms— DBS, halftoning, watermarking

1. INTRODUCTION

In recent years, the technique of digital watermarking has been widely studied since it can be used to establish ownership rights, track content usage, and ensure authorized access, among other applications. However, the watermarks embedded in a digital image may be destroyed if they are printed on paper due to the halftoning process. Watermarking for printed material is a rather fascinating topic with new challenges [1].

Halftone image watermarking is a technique in which the watermark is embedded in the halftoning process by exploiting the characteristics of the halftone image. Because the watermark is directly embedded in the halftone, and the halftone image is robust to the printing and scanning (P&S) process, this technique is, in principle, a very effective approach to printed image watermarking.

There are a number of methods proposed for halftone image watermarking or data hiding. According to the halftoning techniques they employed, most of the methods can be classified into two categories: dithering based method and error-diffusion based method. The basic idea of dithering based methods, e.g. in [2-4], is to embed the watermark using a number of different dither cells in the halftoning process. Methods of this kind have a major advantage of very low computation. But it is difficult to achieve high watermarking capacity. Error diffusion (EDF) is widely used for watermarking (or data hiding) because of its good visual quality and moderate computational complexity. A number of different schemes [5]-[10] have been proposed, and very high watermarking capacity, e.g. 50% in [9], have been reported. Although these schemes can often be effective, they are under pressure to improve image visual quality when the watermarking capacity is high. Some computationally expensive techniques, such as LMS-based halftoning [9][10] and optimized substitution table [10] have been accordingly combined to produce better quality.

In all the error-diffusion based methods, data embedding and visual quality evaluation are two separate processes. This strategy of halftone quality control is essentially an open loop. Therefore, it is not able to ensure optimal performance. In this paper, we will address the problem of halftone image watermarking using direct binary search (DBS) halftoning technique [11]-[13]. DBS tries to minimize the mean squared perceptually filtered error between the continuous-tone image and output halftone image, and it is the most computationally efficient as an iterative process. In addition to significantly better halftone quality, DBS has a more attracting aspect of high flexibility. Since DBS is in nature an optimization process, we can conveniently modify its cost function, or restrict its searching space, or do both, so that halftoning, watermarking, and synchronization pattern insertion (for P-S effect correction) are all taken into account for best performance. In this way, major features of printed image watermarking, such as image quality, watermark capacity, and error detection rate, will be jointly optimized. In [14], a joint halftoning and watermarking scheme based on DBS method has been proposed, however, the original continuous-tone image is required to detect watermark, which largely limits its application. In [15], DBS halftoning is integrated with a scheme utilizing different halftone texture orientations to carry watermark data. However, high capacity cannot be achieved in this method.

The major purpose of this paper is to illustrate a novel joint optimization framework for halftone image watermarking, in which the watermarks are blindly detected

and high capacity can be achieved. In Sec. II, the optimization problem is formulated for combined halftoning, watermarking, and synchronization. In Sec. III, the DBS method is presented to find the optimal solution. Experimental results are given in Sec. IV. Finally, conclusions are given in Sec. V.

2. JOINT OPTIMIZATION OF HALFTONING, WATERMARKING, AND SYNCHRONIZATION

Throughout this paper, we use $[\boldsymbol{m}] = [m, n]$ and $(\boldsymbol{x}) = (x, y)$ to represent discrete and continuous spatial coordinates, respectively. Let $f[\boldsymbol{m}]$ denote the continuous-tone host image, and $g[\boldsymbol{m}]$ the watermarked halftone. It is assumed that both $f[\boldsymbol{m}]$ and $g[\boldsymbol{m}]$ take values between 0 and 1, i.e. $0 \le f[\boldsymbol{m}] \le 1$ and $g[\boldsymbol{m}] = 0$ or 1, where 0 and 1 represent pure black and white, respectively.

In our proposed scheme for halftone image watermarking, three requirements are to be simultaneously satisfied: (i) $g[\boldsymbol{m}]$ has good visual quality as compared to $f[\boldsymbol{m}]$; (ii) watermarks are embedded in $g[\boldsymbol{m}]$ without errors; (iii) synchronization pattern are imperceptibly inserted in $g[\boldsymbol{m}]$. In order to fulfill this task, the pixel indices are grouped into three disjoint sets: set A for information embedding, B for synchronization, and C as the complementary set. In set A, every two pixels form a pair, and this pixel-pair (indexed as $\{\boldsymbol{m}_i, \tilde{\boldsymbol{m}}_i\}$) is forced to be correlated according to its embedded bit $b[i] \in \{0,1\}$ as

$$\left(2g[\boldsymbol{m}_i]-1\right)\left(2g[\tilde{\boldsymbol{m}}_i]-1\right) = 2b[i]-1 \tag{1}$$

All the pixels in B are set to be black, i.e.

$$g[\boldsymbol{m}]=0,\ \forall \boldsymbol{m} \in B \tag{2}$$

and all the black pixels form a pattern used to correct geometrical distortion caused by printing and scanning. The pixels in set C are free, and these pixels, along with those in set A, are to be adjusted for best halftone quality.

In this paper, the visual quality of the halftone is measured by the total squared perceived error between $g[\boldsymbol{m}]$ and $f[\boldsymbol{m}]$ after printing. A human visual system (HVS) model is employed to quantify the perceived error. The definition of HVS-based perceived error is illustrated in Fig. 1, in which the printer is embodied by the printer dot profile $p(\boldsymbol{x})$, and the HVS model [16] is a low-pass linear shift-invariant filter represented by its point spread function $h(\boldsymbol{x})$.

The perceived error between $g[\boldsymbol{m}]$ and $f[\boldsymbol{m}]$ after printing is expressed as

$$\tilde{e}(\boldsymbol{x}) = \tilde{g}(\boldsymbol{x}) - \tilde{f}(\boldsymbol{x}) = \sum_{\boldsymbol{m}} e[\boldsymbol{m}]\tilde{p}(\boldsymbol{x}-\boldsymbol{X}\boldsymbol{m}) \tag{3}$$

where $e[\boldsymbol{m}] = g[\boldsymbol{m}] - f[\boldsymbol{m}]$, $\tilde{p}(\boldsymbol{x}) = p(\boldsymbol{x}) * h(\boldsymbol{x})$ represents the cascading effects of printer rendering and the HVS model, and $\boldsymbol{X}$ is the periodicity matrix whose columns comprise a basis for the lattice of printer addressable dots. The total perceived error can be written as

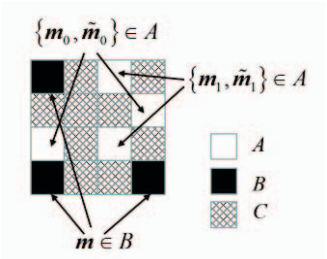

Fig.1 Illustration of three pixel sets for watermarking.

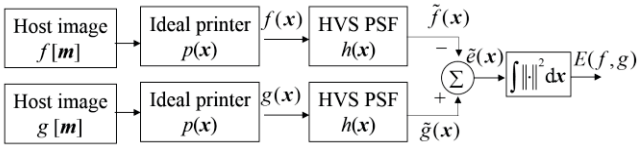

Fig. 2 Definition of HVS-based perceived error.

$$E(f,g) = \int \left|\tilde{e}(\boldsymbol{x})\right|^2 \mathrm{d}\boldsymbol{x} \tag{4}$$

The optimization problem is formulated as

$$\hat{g} = \arg\min_{g} E(f,g),\ \text{s.t. (1) and (2)} \tag{5}$$

i.e. the optimal solution for $g[\boldsymbol{m}]$ is achieved by searching for the minimal value of $E(f, g)$ throughout the restricted binary space defined by (1) and (2).

3. DIRECT BINARY SEARCH IN RESTRICTED BINARY SPACE

By substituting (3) into (4), the total perceived error $E(f, g)$ can be rewritten as [11]

$$E(f,g) = \sum_{\boldsymbol{m}} e[\boldsymbol{m}]c_{\tilde{p}\tilde{e}}[\boldsymbol{m}] \tag{6}$$

where $c_{\tilde{p}\tilde{e}}[\boldsymbol{m}] = c_{\tilde{p}\tilde{e}}(\boldsymbol{X}\boldsymbol{m})$, and $c_{\tilde{p}\tilde{e}}(\boldsymbol{x})$ is the correlation function between $\tilde{p}(\boldsymbol{x})$ and $\tilde{e}(\boldsymbol{x})$

$$c_{\tilde{p}\tilde{e}}(\boldsymbol{x}) = \int \tilde{p}(\boldsymbol{y})\tilde{e}(\boldsymbol{x}+\boldsymbol{y})\mathrm{d}\boldsymbol{y}\,. \tag{7}$$

The correlation $c_{\tilde{p}\tilde{e}}[\boldsymbol{m}]$ can be further evaluated as

$$c_{\tilde{p}\tilde{e}}[\boldsymbol{m}] = \sum_{\boldsymbol{n}} e[\boldsymbol{n}]c_{\tilde{p}\tilde{p}}[\boldsymbol{n}-\boldsymbol{m}], \tag{8}$$

where $c_{\tilde{p}\tilde{p}}[\boldsymbol{m}] = c_{\tilde{p}\tilde{p}}(\boldsymbol{X}\boldsymbol{m})$, and $c_{\tilde{p}\tilde{p}}(\boldsymbol{x})$ is the autocorrelation function of $\tilde{p}(\boldsymbol{x})$ defined by

$$c_{\tilde{p}\tilde{p}}(\boldsymbol{x}) = \int \tilde{p}(\boldsymbol{y})\tilde{p}(\boldsymbol{y}+\boldsymbol{x})\mathrm{d}\boldsymbol{y}\,. \tag{9}$$

In DBS, only two kinds of trial pixel changes, i.e. toggle and swap, are considered. Toggle means only the current pixel is to be changed, from 1 to 0, or 0 to 1. In swap, both the current pixel and one of its 8 nearest neighbor pixels that has a different value are to be changed.

1) *Toggle and swap in set C*

The free pixels in set C are to be toggled and swapped as in normal DBS-based halftoning [11]. Let $g[\boldsymbol{n}_0]$ and $g[\boldsymbol{n}_1]$ represent the current pixel and one of its neighbors, both of

which belong to C, the trial change of swap or toggle can be expressed as

$$g'[\boldsymbol{m}] = g[\boldsymbol{m}] + a_0\delta[\boldsymbol{m}-\boldsymbol{n}_0] + a_1\delta[\boldsymbol{m}-\boldsymbol{n}_1] \quad (10)$$

where $a_0 = 1-2g[\boldsymbol{m}_0]$, $a_1 = 0$ for toggle, and $a_1 = -a_0$ for swap. For the trial change of (10), the change in total squared error is derived as

$$\begin{aligned}\Delta E &= E(f,g') - E(f,g) \\ &= (a_0^2 + a_1^2)c_{\tilde{p}\tilde{p}}[0] + 2a_0a_1c_{\tilde{p}\tilde{p}}[\boldsymbol{n}_1-\boldsymbol{n}_0] + \\ &\quad 2a_0c_{\tilde{p}\tilde{e}}[\boldsymbol{n}_0] + 2a_1c_{\tilde{p}\tilde{e}}[\boldsymbol{n}_1]\end{aligned} \quad (11)$$

If $\Delta E < 0$, this trial change of toggle or swap will be accepted, and $c'_{\tilde{p}\tilde{e}}$ is updated as follows

$$c'_{\tilde{p}\tilde{e}}[\boldsymbol{m}] = c_{\tilde{p}\tilde{e}}[\boldsymbol{m}] + a_0c_{\tilde{p}\tilde{p}}[\boldsymbol{m}-\boldsymbol{n}_0] + a_1c_{\tilde{p}\tilde{p}}[\boldsymbol{m}-\boldsymbol{n}_1] \quad (12)$$

2) *Pair toggle in set A*

As for $\boldsymbol{m}_i \in A$, because of the constraint of pixel-correlation embedding condition, only a special trial change of pair-toggle is permitted, which is defined as

$$g'[\boldsymbol{m}] = g[\boldsymbol{m}] + a_0\delta[\boldsymbol{m}-\boldsymbol{m}_i] + a_1\delta[\boldsymbol{m}-\tilde{\boldsymbol{m}}_i] \quad (13)$$

where $\boldsymbol{m}_i$ and $\tilde{\boldsymbol{m}}_i$ form a pixel-pair to embed the information bit b_i, $a_0 = 1-2g[\boldsymbol{m}_i]$, and $a_1 = 1-2g[\tilde{\boldsymbol{m}}_i] = (2b_i-1)a_0$. For this trial change, ΔE and $c'_{\tilde{p}\tilde{e}}$ are derived as

$$\begin{aligned}\Delta E = {} & 2a_0\left(c_{\tilde{p}\tilde{e}}[\boldsymbol{m}_i] + (2b_i-1)c_{\tilde{p}\tilde{e}}[\tilde{\boldsymbol{m}}_i]\right) + \\ & 2\left(c_{\tilde{p}\tilde{p}}[0] + (2b_i-1)c_{\tilde{p}\tilde{p}}[\boldsymbol{m}_i-\tilde{\boldsymbol{m}}_i]\right)\end{aligned} \quad (14)$$

$$\begin{aligned}c'_{\tilde{p}\tilde{e}}[\boldsymbol{m}] = {} & c_{\tilde{p}\tilde{e}}[\boldsymbol{m}] + \\ & a_0\left(c_{\tilde{p}\tilde{p}}[\boldsymbol{m}-\boldsymbol{m}_i] + (2b_i-1)c_{\tilde{p}\tilde{p}}[\boldsymbol{m}-\tilde{\boldsymbol{m}}_i]\right)\end{aligned} \quad (15)$$

The whole process of watermarking can be formulated in the following steps:

1) First, in the initialization step, all the pixel-pairs in A are forced to be correlated according to the embedded bits, as defined in (1), and the pixels in B are set to black. These restrictions will be strictly satisfied in the subsequent steps.

2) Second, during pixel-by-pixel scanning, $E(f, g)$ is to be minimized. For pixels in B, no change is permitted. For pixels in C, each trial change is evaluated according to (11), and updated with (10) and (12) if the trial change is accepted. As for pixels in A, the trial change of (13) is evaluated according to (14), and (15) is updated if the trial change is accepted.

3) Third, the pixel-by-pixel scanning is executed iteratively until the convergence of $E(f,g)$ is achieved, which is defined as the point at which no trial change are accepted during a complete pass through the image.

4. EXPERIMENTS AND RESULTS

The flow chart of the experiments is illustrated in Fig.3. We demonstrate our results on the host images of Lena, Peppers, Boat and Mandrill of size 512×512 pixels, which are shown in Fig. 4 (a) - (d). The watermark key P is used to generate

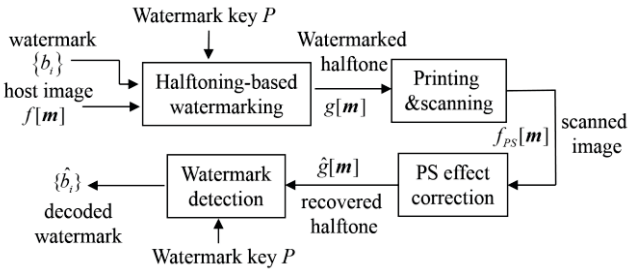

Fig. 3 Flow chart of experiments.

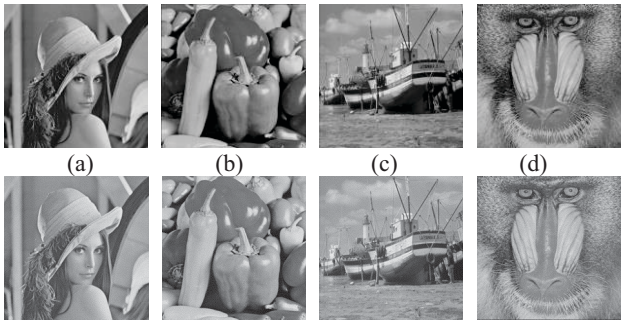

Fig. 4 Images of Lena, Peppers, Boat, and Mandrill. (a)-(d), original grayscale image; (e)-(h), DBS halftones.

Fig. 5 Graphic pattern for P&S distortion correction.

pseudo-random numbers determining the pixel-pair location $\{\boldsymbol{m}_i, \tilde{\boldsymbol{m}}_i\}$ for each b_i. For the sake of P&S distortion correction, 2785 black pixels (about 1% of the total number of pixels) forming a pattern, shown in Fig. 6, is inserted in the watermarked halftone. This pattern is rather imperceptible when hidden in the halftone, and its 8 vertical and 15 horizontal black dotted lines are very effective dealing with the global nonlinear geometric distortions. Due to space limitation, we do not describe the P&S Effect Correction procedure in this paper.

In order to get reasonable values representing halftone quality, we calculate the normalized HVS mean squared value (NMSE) as

$$\text{NMSE} = -10\log_{10}\frac{E(f,g)}{MNc_{\tilde{p}\tilde{p}}[0]} \ \text{(dB)} \quad (16)$$

where $M\times N$ denotes the size in pixels of the image. The DBS halftones of Fig. 4(a)-(d) without watermark are shown in Fig. 4(e)-(h), respectively. Here, the NMSE values are 24.7 dB(Lena), 24.6 dB (Peppers), 24.6 dB(Boat), and 24.7 dB (Mandrill).

In dithering based or error-diffusion based works, peak signal to noise ratio (PSNR) is evaluated to measure the quality of the halftone. The definition of PSNR is written as

(a) (b) (c) (d)

Fig. 6 Bitmap logos to be embedded (a) 110×110 pixels, (b)160×160 pixels, (c) 270×270 pixels, and (d) 350×350 pixels

$$\mathrm{PSNR} = 10\log_{10}\frac{M\times N}{\sum_{m=1}^{M}\sum_{m=1}^{N}\left\{f[m,n]-\sum_{i,j}w_{i,j}g[m+i,n+j]\right\}^2} \quad (17)$$

where $w_{i,j}$ denotes human visual filter. The filter $\{w_{i,j}\}$ can be derived as least mean squared (LMS) filter by training sets of gray-level images and their good halftone results, as recommended in [8]. In this paper we will also calculate the values of PSNR for reference. The derived LMS filter of size 7×7 from the host images Fig. 4(a)-(d) and their DBS halftones (Fig 4. (e)-(h)) is listed in Table I, and the PSNR values of these original halftones are 30.5dB (Lena), 30.5dB (Peppers), 27.7dB (Boat), and 22.6dB (Mandrill).

The performances are represented by watermark rate (WMR), halftone recovering pixel error rate (PER), watermark decoding bit error rate (BER), NMSE, and PSNR. Four bitmap images as shown in Fig. 6 are to be embedded as watermarks. These marks have the sizes of 110×110, 160×160, 270×270, and 350×350 pixels, which correspond to the watermark rates of 4.62%, 9.77%, 27.81%, and 46.73% respectively. The halftone is printed at 200 dpi and scanned at 600 dpi by an HP Deskjet Ink Print &Scan 3548. The experimental results for NMSE, PSNR, PER, and BER are listed in Table II, the watermarked halftone with very high WMR (i.e. 46.7%) are shown in Fig. 7, and a group of samples of recovered halftone and decoded watermarks are shown in Fig. 8 and Fig. 9, respectively.

The experimental results demonstrate excellent performance of our proposed scheme. We find that the degradation of halftone quality is negligible when WMR is below 10%, and the halftone quality remains pretty good even for so high WMR as WMR = 46.7% (as shown in Fig. 7). Since the watermarks are embedded in the halftone without errors, the error decoding rate highly depends on the performance of the P&S recovery. Both PER and BER are very low (about 1%) in all the experiments, and there is a general rule that BER tends to increase to be twice that of PER when WMR grows very high (e.g. 46.7%).

5. CONCLUSION

In this paper, we present a novel framework for printed image watermarking, which is a combined process that halftoning, data embedding, and synchronization pattern insertion are done simultaneously. Excellent performances of both excellent visual quality and high watermark capacity are verified by the experiments.

TABLE I
LMS FILTER FROM DBS HALFTONES $w_{i,j}$ (10^{-2})

-0.66	-0.55	0.28	0.83	0.40	-0.39	-0.55
-0.67	0.32	2.55	3.85	2.74	0.56	-0.51
-0.07	2.19	6.01	8.04	6.16	2.38	0.04
0.35	3.29	7.81	10.09	7.84	3.32	0.37
0.05	2.41	6.19	8.09	6.09	2.28	-0.03
-0.49	0.62	2.81	3.92	2.65	0.42	-0.61
-0.53	-0.34	0.45	0.87	0.33	-0.48	-0.62

TABLE II
EXPERIMENTAL RESULTS

Host Image	WMR	NMSE (dB)	PSNR (dB)	PER	BER
Lena	4.62%	24.5	30.3	0.79%	0.73%
	9.77%	24.4	30.2	0.97%	0.80%
	27.81%	20.9	28.0	0.70%	0.80%
	46.73%	17.6	25.5	0.58%	1.13%
Peppers	4.62%	24.5	30.4	1.19%	1.50%
	9.77%	24.2	30.3	1.70%	1.85%
	27.81%	20.9	28.1	1.30%	1.36%
	46.73%	17.6	25.6	1.20%	2.34%
Boat	4.62%	24.5	27.7	1.32%	1.15%
	9.77%	24.3	27.6	1.42%	0.97%
	27.81%	20.8	26.0	1.23%	1.20%
	46.73%	17.5	24.2	0.90%	1.74%
Mandrill	4.62%	24.5	22.5	0.31%	0.38%
	9.77%	24.4	22.5	0.43%	0.51%
	27.81%	20.7	21.8	0.31%	0.41%
	46.73%	17.7	21.0	0.26%	0.52%

(a) (b) (c) (d)

Fig. 7 Watermarked halftone with WMR=46.7%.

(a) (b) (c) (d)

Fig. 8 Recovered watermarked halftones of Peppers. The water mark rates are: (a) 4.62%, (b) 9.77%, (c) 27.8%, and (d) 46.7%.

(a) (b) (c) (d)

Fig. 9 Decoded watermarks, from Fig. 8 (a)-(d), respectively.

6. REFERENCES

[1] Borko Furht, Darko Kirovski., *Multimedia Watermarking Techniques and Applications*, Taylor & Francis Group, LLC, 2006

[2] K. T. Knox and S. G. Wang, "Digital Watermarks Using Stochastic Screens," *Proc. SPIE*, vol. 3018, 1997.

[3] Z. Baharav and D. Shaked, "Watermarking of Dithered Halftone Images, " *Proc. SPIE*, vol. 3657, 1999.

[4] H. Z. Hel-Or, "Watermarking and Copyright Labeling of Printed Images," *Journal of Electronic Imaging*, vol.10, no. 3, pp. 794-803, Jul. 2001

[5] M. S. Fu and O. C. Au, "Data Hiding Watermarking for Halftone Images," *IEEE Transactions on Image Processing*, vol.11, no. 4, pp. 477-484, Apr. 2002

[6] M. S. Fu and O. C. Au, "Steganography in Halftone Images: Conjugate Error Diffusion," *Signal Processing*, vol. 83, no. 10, pp. 2171-2178, 2003

[7] S. C. Pei and J. M. Guo, "Data Hiding in Halftone Images with Noise-balanced Error Diffusion," *IEEE Signal Processing Letters*, vol. 10, no. 12, pp. 349-351, Dec. 2003

[8] S. C. Pei and J. M. Guo, "High-Capacity Data Hiding in Halftone Images Using Minimal-Error Bit Searching and Least-Mean Square Filter," *IEEE Transactions On Image Processing*, vol.15, no. 8, pp. 2441-2453, Jun. 2006

[9] J. M. Guo and Y. F. Liu, "Halftone-Image Security Improving Using Overall Minimal-Error Searching," *IEEE Transactions on Image Processing*, vol. 20, no. 10, pp. 2800-2812, Oct. 2011

[10] J. M. Guo, S. C. Pei, and H. Lee, "Watermarking in Halftone Images with Parity-Matched Error Diffusion," *Signal Processing*, vol.91, no. 1, pp. 126-135, 2011

[11] M. Analoui and J. P. Allebach, "Model-Based Halftoning using Direct Binary Search," *Proc. SPIE*, vol. 1666, 1992.

[12] D. J. Lieberman and J. P. Allebach, "A dual Interpretation for Direct Binary Search and Its Implications for Tone Reproduction and Texture Quality," *IEEE Transactions on Image Processing*, vol. 9, pp. 1950–1963, Nov. 2000.

[13] S. H. Kim, and J. P. Allebach, "Impact of HVS Models on Model-Based Halftoning," *IEEE Transactions on Image Processing*, vol. 11, No. 3, pp. 258-269, 2002

[14] D. Kacker and J. P. Allebach, "Joint Halftoning and Watermarking," *IEEE Transactions on Signal Processing*, vol. 51, no. 4, pp. 1054-1068, Apr. 2003.

[15] J. M. Guo, C. C. Su, Y. F. Liu, et al., "Oriented Modulation for Watermarking in Direct Binary Search Halftone Images," *IEEE Transactions on Image Processing*, vol. 21, no. 9, pp. 4117-4127, Sep. 2012.

[16] R. Näsänen, "Visibility of halftone dot textures," *IEEE Transactions on Systems, Man, and Cybernetics: Systems*, vol. 14, no. 6, pp. 920–924, 1984.